Comprehensive Study of the Third-order Charge Pump PLL Dynamic Behavior

Hannane Gholamnataj[1], Habib Adrang[2]
1- Department of Electrical Engineering, Nour Branch, Islamic Azad University, Nour, Iran
Email: hannane.nataj@gmail.com
2- Department of Electrical Engineering, Nour Branch, Islamic Azad University, Nour, Iran
Email: habibadrang@gmail.com (Corresponding author)

Received: Nov. 1 2013 Revised: Dec. 5 2013 Accepted: Jan. 2 2014

ABSTRACT:
This paper provides useful equations for the analysis of loop dynamics specification such as damping ratio, overshoot and settling time in the third-order charge pump PLL with second-order loop filter. The presented analysis method is based on the approximation of the output phase step response using the step response of the second-order systems. In fact, the results can be used as an accurate approximation in the design and analysis of third-order PLL. The performance of this method has been verified in an interesting example using behavioral simulations in MATLAB. Simulations demonstrate a significant agreement between the simulated results of the actual PLL and the proposed approximated approach.

KEYWORDS: Phase Locked Loop (PLL), Charge Pump (CP), Phase Detector (PD), Settling time(t_s), Damping ratio (ξ), Overshoot, Peak time, Rise time(t_r).

1. INTRODUCTION

Phase Locked Loops (PLLs) are widely used as clock generators in a variety of applications including microprocessors, wireless receivers, serial link transceivers, and disk drive electronics [1]-[9]. They are generally used in clock recovery and frequency synthesizing of wireless communication systems. The stability characteristics, bandwidth and fast locking time are the PLL's important specifications in high speed communication systems. For example, a wider loop bandwidth directly translates to a faster locking, and hence, the bandwidth must be maximized to minimize the lock time.

While there are numerous PLL design examples in the literature, a precise analysis and mathematical clarity of the loop dynamics of the PLL is lacking. The two most popular references in this arena by Hein and Scott [10] and Gardner [11] provide useful insight to analysis of second-order PLLs. Several other references [12], [13], provide simplified yet useful approximations of third-order PLLs. However, they do not provide a complete and extensive analysis for practical integrated circuit of PLLs, i.e., third-order PLLs. Extension to higher orders such as type II third-order PLL is still a topic of interest among researchers and cannot be solved analytically as easily as the second-order PLL mainly because there is an additional pole in transfer function that degrades the phase margin and causes peaking in the frequency response. Hence, we need to seek a method to determine the optimum location of this pole [14]. The frequency analysis of third-order PLL has been presented in several papers [15], [16], but the transient analysis is not investigated. Recently, we studied the damping ratio, phase margin and settling time of the third-order PLL [17], [18]. But, a comprehensive design method covering all of the dynamic behavior parameters like overshoot, rise time etc. is still missing among the previously presented works.

The aim of this paper is to give insightful understanding of the PLL dynamics. In particular, it is of interest to analyze the transient behavior of the PLL and derive accurate and useful expressions for estimating the time-domain response parameters such as settling time, damping ratio and overshoot. The focus of the detailed derivations and analysis is on the Charge pump PLL (CPLL) because IC designers predominantly choose CPLLs over other PLL architectures. Although the presentation is for a CPLL, the analysis can be readily extended for other PLL architectures. Since the PLL with second-order loop filter is widely used in practical implementations, this paper concentrates on the analysis of PLLs with second-order loop filter.

The paper is organized as follows. The system level modeling of the third-order charge pump PLL is presented in Section 2. In sections 3 and 4, the transient response solutions of PLL are presented and closed-form expressions are derived for settling time, overshoot and damping ratio estimation. In section 5, the presented analysis is verified through an example and behavioral simulations in MATLAB. Finally, the paper is concluded in section 6.

2. THIRD-ORDER CHARGE PUMP PLL ARCHITECTURE

Fig. 1 shows the systematic model of a PLL with second-order loop filter [17]-[19]. A conventional charge third-order pump PLL consists of a phase frequency detector (PFD), a charge pump (CP), a loop filter (LF) and a voltage controlled oscillator (VCO). The charge pump consists of two switched current sources that pump charge into or out of the loop filter. The phase or the frequency of the reference (V_{in}) and feedback (V_{out}) signals are compared with the PFD and any difference will be translated to a current in the charge pump (I_P). These analog current pulses are integrated and converted to voltage V_{cont} through the loop filter. The noise and the high frequency components in the charge pump output will be removed by the loop filter consisting of R_P, C_P and C_2. The output signal of the loop filter drives the VCO which generates a signal with a specific frequency depending on the control voltage (V_{cont}). The capacitor C_2 is used to improve the transient characteristics by suppressing the sudden jumps of the VCO control voltage (V_{cont}) caused by charge injection and clock feed through of the two switches. This capacitor is usually much smaller than C_P. The phase-domain model of the PLL is shown in Fig. 2. This model is used as a behavioral prototype in system level simulations to verify the derived expressions. Fig. 3 shows the alternative phase-domain model where, K_{VCO} is the VCO gain, $b=1+C_P/C_2$ and I_P is the charge pump current. From Fig. 3, the closed loop transfer function of the third-order PLL is given as [20]

$$H(s)\big|_{close} = \frac{C(s)}{R(s)} = \frac{K_v b s + \dfrac{K_v b}{R_P C_p}}{s^3 + \dfrac{b}{R_P C_p} s^2 + K_v b s + \dfrac{K_v b}{R_P C_p}} = \frac{b_1 s + b_0}{s^3 + b_2 s^2 + b_1 s + b_0} \tag{1}$$

Where,

$$K_v = I_p K_{VCO} / [2\pi (C_2 + C_p)] \tag{2}$$

$$b_0 = K_v b / (R_P C_P) \tag{3}$$

$$b_1 = K_v b \tag{4}$$

$$b_2 = b / (R_P C_P) \tag{5}$$

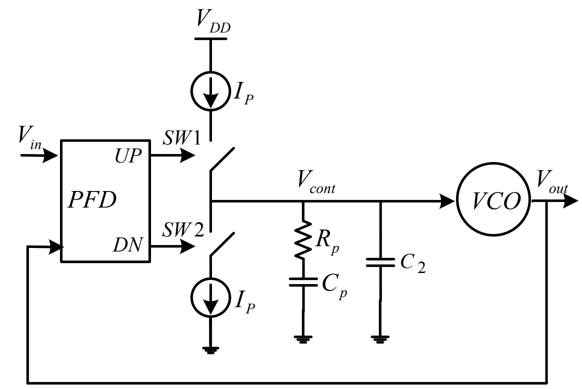

Fig. 1. Structure of the PLL with second-order loop filter

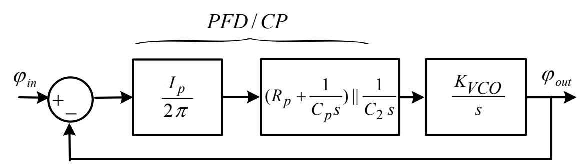

Fig. 2. Phase domain model of the PLL

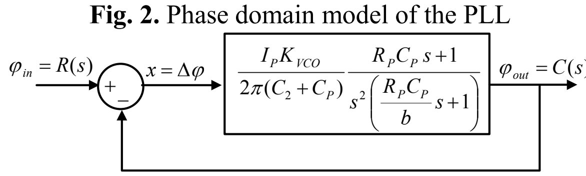

Fig. 3. Phase domain structure of the PLL

The phase margin of the third-order PLL can be obtained as follows [18]

$$\tan(PM) = \frac{(1 - 1/b) K_v (R_p C_p)^2}{1 + K_v^2 (R_p C_p)^4 / b} \tag{6}$$

The maximum obtainable phase margin is only a function of b and can be calculated as follows [19]

$$PM\big|_{\max} = \tan^{-1}\left[\frac{1}{2}\left(\frac{b-1}{\sqrt{b}}\right)\right] \tag{7}$$

As seen in (7), the phase margin will be increased by increasing b or C_p/C_2 ratio. Thus, the loop stability will be reduced if b is decreased. It is indicated in [19] that the phase margin will be maximized if (8) is satisfied.

$$K_v(R_pC_p)^2 = \sqrt{b} \qquad (8)$$

For the unit-step input $R(s) = 1/s$, the output $C(s)$ is

$$C(s) = \frac{b_1 s + b_0}{s(s^3 + b_2 s^2 + b_1 s + b_0)} \qquad (9)$$

The inverse Laplace transform calculation of the $C(s)$ is very complicated. So, the analysis of loop dynamics specifications is difficult. In this paper, new closed form equations are proposed for dynamic specifications such as phase margin, damping ratio, overshoot and settling time.

3. THE PROPOSED APPROACH FOR TRANSIENT ANALYSIS

In this section, the transient response characteristics of the third-order PLL are approximated through the transient response of a second-order system. As known, the unit step response of second order systems can be described as follows [21]

$$c_1(t) = 1 - (e^{-\alpha t} / \beta)\sin(\omega_d t + \theta) \qquad (10)$$

Where, α is called the attenuation and ω_d is the damped natural frequency of the system. The transient response of a practical control system often exhibits damped oscillation before steady state. A unit step response curve of a typical second-order system is shown in Fig. 4. In order to specify the transient response characteristic of a control system to a unit-step input, it is common to specify the followings

1. Rise time, t_r
2. Maximum overshoot, M_p
3. Settling time, t_s
4. Peak time, t_p

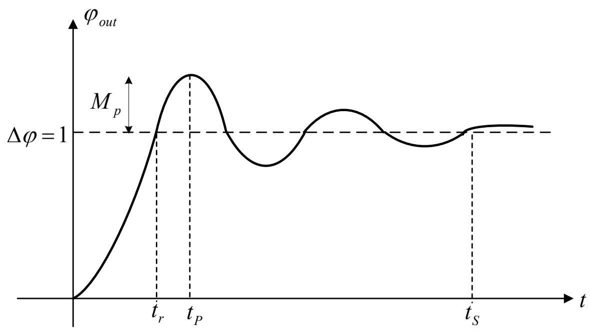

Fig. 4. Unit-step response curve showing t_r, t_p, M_p and t_s

The proposed approach is based on approximating the phase step response of the third-order PLL by the step response of the second order systems. In this approach, an additional parameter t_d is introduced to obtain an extra degree of freedom. Therefore, the transient response is approximated by (11).

$$c_o(t) = 1 - (e^{-\alpha(t+t_d)} / \beta)\sin[\omega_d(t + t_d) + \theta] \qquad (11)$$

Where, t_d is the new introduced parameter. The dynamic behavior of the system can then be described in terms of four parameters α, β, θ and ω_d. Thus, the Laplace transform of $c_o(t)$ can be written in terms of Laplace transform of $c_1(t)$ as follows

$$C_o(s) = L[c_o(t)] = L[c_1(t + t_d)] = e^{st_d} L[c_1(t)] \qquad (12)$$

Firstly, the Laplace transform of $c_1(t)$ is calculated. Equation (10) can be rewritten as

$$c_1(t) = 1 - \frac{1}{\beta} e^{-\alpha t}[\sin(\omega_d t)\cos\theta + \cos(\omega_d t)\sin\theta] \qquad (13)$$

Then, the Laplace transform of $c_1(t)$ is obtained as

$$C_1(s) = \frac{1}{s} - \frac{\cos\theta}{\beta}\frac{\omega_d}{(s+\alpha)^2 + \omega_d^2} - \frac{\sin\theta}{\beta}\frac{s+\alpha}{(s+\alpha)^2+\omega_d^2}$$
$$= \frac{(1 - \frac{\sin\theta}{\beta})s^2 + (2\alpha - \frac{\cos\theta}{\beta}\omega_d - \frac{\sin\theta}{\beta}\alpha)s + \alpha^2 + \omega_d^2}{s[(s+\alpha)^2 + \omega_d^2]} \qquad (14)$$

The transfer function of $C_1(s)$ can be simplified, yielding

$$C_1(s) = \frac{a_2 s^2 + a_1 s + a_0}{s[(s+\alpha)^2 + \omega_d^2]} = \frac{a_2 s^2 + a_1 s + a_0}{s(s^2 + 2\alpha s + a_0)} \qquad (15)$$

Where

$$a_0 = \alpha^2 + \omega_d^2 \qquad (16)$$

$$a_1 = 2\alpha - \frac{1}{\beta}\cos\theta\,\omega_d - \frac{\alpha}{\beta}\sin\theta \qquad (17)$$

$$a_2 = 1 - \frac{\sin\theta}{\beta} \qquad (18)$$

Referring to (12), we have

$$C_o(s) = e^{st_d} C_1(s) = e^{st_d}\frac{a_2 s^2 + a_1 s + a_0}{s(s^2 + 2\alpha s + a_0)} \qquad (19)$$

Equation (19) is an approximation of the $C(s)$ output. Equating $C(s)$ and $C_o(s)$ from (9) and (19), respectively, results in

$$
\begin{aligned}
&e^{st_d}\,\frac{a_2s^2+a_1s+a_0}{s(s^2+2\alpha s+a_0)}=\frac{b_1s+b_0}{s(s^3+b_2s^2+b_1s+b_0)}\\
&\Rightarrow \frac{a_2s^2+a_1s+a_0}{e^{-st_d}(s^2+2\alpha s+a_0)}=\frac{b_1s+b_0}{s^3+b_2s^2+b_1s+b_0}
\end{aligned}
\tag{20}
$$

The delay time t_d is very small and therefore e^{-st_d} is frequently approximated by

$$e^{-st_d}=1-st_d \tag{21}$$

Substituting (21) in to (19) results in (22)

$$\frac{a_2s^2+a_1s+a_0}{(1-st_d)(s^2+2\alpha s+a_0)}\approx\frac{b_1s+b_0}{s^3+b_2s^2+b_1s+b_0} \tag{22}$$

Comparing numerators in both sides of (22) results in

$$a_2=0 \;\Rightarrow\; 1-\frac{\sin\theta}{\beta}=0 \;\Rightarrow\; \beta=\sin\theta \tag{23}$$

Then rearranging (22) yields

$$
\begin{aligned}
C_o(s)&=\frac{a_1s+a_0}{-t_ds^3+(1-2\alpha t_d)s^2+(2\alpha-a_0t_d)s+a_0}\\
&=\frac{\frac{a_1}{-t_d}s+\frac{a_0}{-t_d}}{s^3+\frac{(1-2\alpha t_d)}{-t_d}s^2+\frac{(2\alpha-a_0t_d)}{-t_d}s+\frac{a_0}{-t_d}}\\
&=\frac{b_1s+b_0}{s^3+b_2s^2+b_1s+b_0}=C(s)
\end{aligned}
\tag{24}
$$

By comparing coefficients of s^3, s^2, s^1, and s^0 terms on both sides of the (24), we get

$$\frac{-a_1}{t_d}=b_1 \quad\Rightarrow\quad a_1=-b_1t_d \tag{25}$$

$$\frac{-a_0}{t_d}=b_0 \quad\Rightarrow\quad a_0=-b_0t_d \tag{26}$$

$$b_2=\frac{1-2\alpha t_d}{-t_d} \quad\Rightarrow\quad 2\alpha t_d=1+b_2t_d \tag{27}$$

$$b_1=\frac{2\alpha-a_0t_d}{-t_d} \quad\Rightarrow\quad -b_1t_d=2\alpha-a_0t_d \tag{28}$$

Substituting (26) and (27) in to (28) we have

$$b_0t_d^3+b_1t_d^2+b_2t_d+1=0 \tag{29}$$

Using (29), the real negative value of t_d can be obtained. Then, referring to (25), (26) and (27) the values of a_1, a_0 and α will be calculated respectively. Also from (16), we have

$$\omega_d=\sqrt{a_0-\alpha^2} \tag{30}$$

Substituting (23) in to (17) gives

$$\tan\theta=\frac{\omega_d}{a_1-\alpha} \tag{31}$$

Therefore, θ can be calculated from (31).

4. TRANSIENT RESPONSE SPECIFICATIONS

In the following, the rise time, peak time, maximum overshoot and settling time of the third-order PLL will be calculated using the approximated transient response given by (11).

Rise time t_r: The rise time is the required time for the response to rise from 0% to 100% of its final value. Referring to (11), the rise time can be calculated by letting $c(t_r)=1$. This means

$$\omega_d(t_r+t_d)+\theta=0 \tag{32}$$

Thus, the rise time t_r is

$$t_r=\frac{-\theta}{\omega_d}-t_d \tag{33}$$

Settling time t_s: The settling time is the time required for the response curve to reach and stay within a specified error around the final value by absolute percentage of it (usually ±2% or ±5%). The curves $\hat{c}(t)=1\pm(e^{-\alpha(t+t_d)}/\beta)$ are the envelopes of the transient response of the unit-step input. The response curve $c(t)$ always remains within a pair of the envelope curves. If the ±5% criterion is used then t_s will be obtained as follow.

$$
\begin{aligned}
&\hat{c}(t_s)=1-\frac{e^{-\alpha(t_s+t_d)}}{\beta}=1.05\\
&\Rightarrow\quad t_s=\frac{\ln(-0.05\beta)}{-\alpha}-t_d
\end{aligned}
\tag{34}
$$

Peak time t_p: The peak time is the time required for the response to reach the first peak of the overshoot. It can be obtained by differentiating $c(t)$ with respect to time and letting it equal to zero. Knowing the fact that the time derivative of the unit-step response is the unit-impulse response, the impulse response should be calculated and set to zero. Referring to (19), for the unit-impulse input $R(s)=1$, the output $H_1(s)$ becomes

$$H_1(s)=e^{st_d}\,\frac{a_1s+a_0}{s^2+2\alpha s+a_0}=e^{st_d}H_2(s) \tag{35}$$

Where

$$H_2(s) = \frac{a_1 s + a_0}{s^2 + 2\alpha s + a_0} = \frac{a_1(s+\alpha-\alpha)+a_0}{(s+\alpha)^2+\omega_d^2} = \frac{a_1(s+\alpha)}{(s+\alpha)^2+\omega_d^2} + \frac{a_0 - a_1\alpha}{\omega_d}\frac{\omega_d}{(s+\alpha)^2+\omega_d^2} \quad (36)$$

The inverse Laplace transform of this equation yields the time solution for the response $h_2(t)$ as follows

$$h_2(t) = a_1 e^{-\alpha t}\cos(\omega_d t) + \frac{a_0 - a_1\alpha}{\omega_d} e^{-\alpha t}\sin(\omega_d t) = A e^{-\alpha t}\sin(\omega_d t + \phi) \quad (37)$$

Where

$$A = \sqrt{a_1^2 + \frac{(a_0 - a_1\alpha)^2}{\omega_d^2}} \quad (38)$$

$$\phi = \tan^{-1}\frac{a_1\omega_d}{a_0 - a_1\alpha} \quad (39)$$

Using (25) and (26) in (39) yields

$$\phi = \tan^{-1}\frac{-b_1 t_d \omega_d}{-b_0 t_d + b_1 t_d \alpha} = \tan^{-1}\frac{b_1\omega_d}{b_0 - b_1\alpha} \quad (40)$$

The peak time is obtained by letting impulse response equal to zero. Therefore, from (35) and (37) we get

$$h_1(t) = h_2(t + t_d) = A e^{-\alpha(t+t_d)}\sin[\omega_d(t+t_d)+\phi] = 0 \quad (41)$$

Since the peak time corresponds to the first peak overshoot, (41) yields the following equation

$$\omega_d(t_p + t_d) + \phi = 0 \quad \Rightarrow \quad t_p = \frac{-\phi}{\omega_d} - t_d \quad (42)$$

Maximum overshoot M_p: The maximum overshoot occurs at the peak time. Assuming that the final value of the output is unity, *Mp* is obtained from (11) and (42) as

$$M_P = c(t_P) - 1 = -(e^{-\alpha(t_P+t_d)}/\beta)\sin[\omega_d(t_P+t_d)+\theta] = -\frac{e^{-\alpha(\frac{-\phi}{\omega_d})}}{\beta}\sin(-\phi+\theta) = \frac{e^{(\frac{\alpha\phi}{\omega_d})}}{\beta}\sin(\phi-\theta) \quad (43)$$

The maximum overshoot of the second-order system can be calculated from the following equation

$$M_{P2} = e^{-\frac{\pi\xi}{\sqrt{1-\xi^2}}} \quad (44)$$

Where, ξ is called the damping ratio. Thus, from (43) and (44) the equivalent damping ratio of the third-order PLL can be approximated as

$$\ln(M_P) = -\frac{\pi\xi}{\sqrt{1-\xi^2}} \quad \Rightarrow \quad \xi = \frac{-\ln M_P}{(\ln M_P)^2 + \pi^2} \quad (45)$$

5. TRANSIENT RESPONSE SPECIFICATIONS

In order to determine the validity of the proposed method for the analysis of third order PLL, a test bench was created using the MATLAB simulator and an interesting example is carefully expressed and simulation is used to compare the results from theoretical analysis and simulation of actual PLL. The corresponding loop parameters are designed to reach phase margin equal to 60˚. As a result, from (7), *b=13.9*. Assuming that C_p*=300pf*, then C_1*=23.2 pf*. Also, if R_p*=2KΩ*, using (8), K_V *= 1.035e13*. Knowing the VCO gain, the charge pump current I_p can be easily obtained from (2). Assuming $K_{VCO}=50\times10^6$ *Hz/V*, I_p*=420µA*.
By the set of equations (3)-(5), we have

$b_1 = K_V\, b$=1.44e14

$b_0 = b_1 / (R_pC_p)$ = 2.4e20

$b_2 = b / (R_pC_p)$ =2.32e7

Equation (29) can be solved using MATLAB to obtain t_d and a_1, a_0 and α are calculated referring to equations (25)-(27). Also, ω_d, θ and β are obtained by (30), (31) and (23), respectively. Note that the transient parameters are obtained by the set of equations (33), (34), (39), (42), (43) and (45). To verify the precision of the introduced approach in section 3 and 4, (11) is plotted in Fig. 5 for the parameters outlined above, where the horizontal axis is time and the vertical axis is the output phase. Also, the phase unit-step response of the third-order PLL has been simulated in MATLAB and is demonstrated in Fig. 5. The results predicted by (11) are observed to precisely match the results obtained via simulation (dashed lines of the Fig. 5). As seen, the precision of the match is such that the simulation based curves and the prediction based curves are nearly indistinguishable in the figure. Table 1 summarizes the parameters of this example.
The proposed approach for calculating of the transient specifications of the PLL is evaluated by simulations for different values of I_p, R_p and C_2. The calculated rise time, settling time and overshoot from (33), (34) and (43) for different values of C_2, R_p and I_P are compared with the simulation results as shown in Fig. 6. In this example, the value of C_2 is swept from *30pf* to *100pf* with the constant values of other parameters. Also, in similar way, R_p and I_p are swept from *2KΩ* to *5KΩ* and *420µA* to *650µA*, respectively.

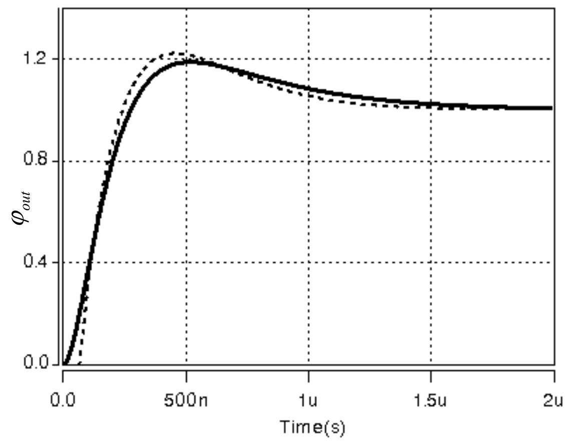

Fig. 5. The actual (solid lines) and approximated (dashed lines) unit-step response of the designed 3rd PLL

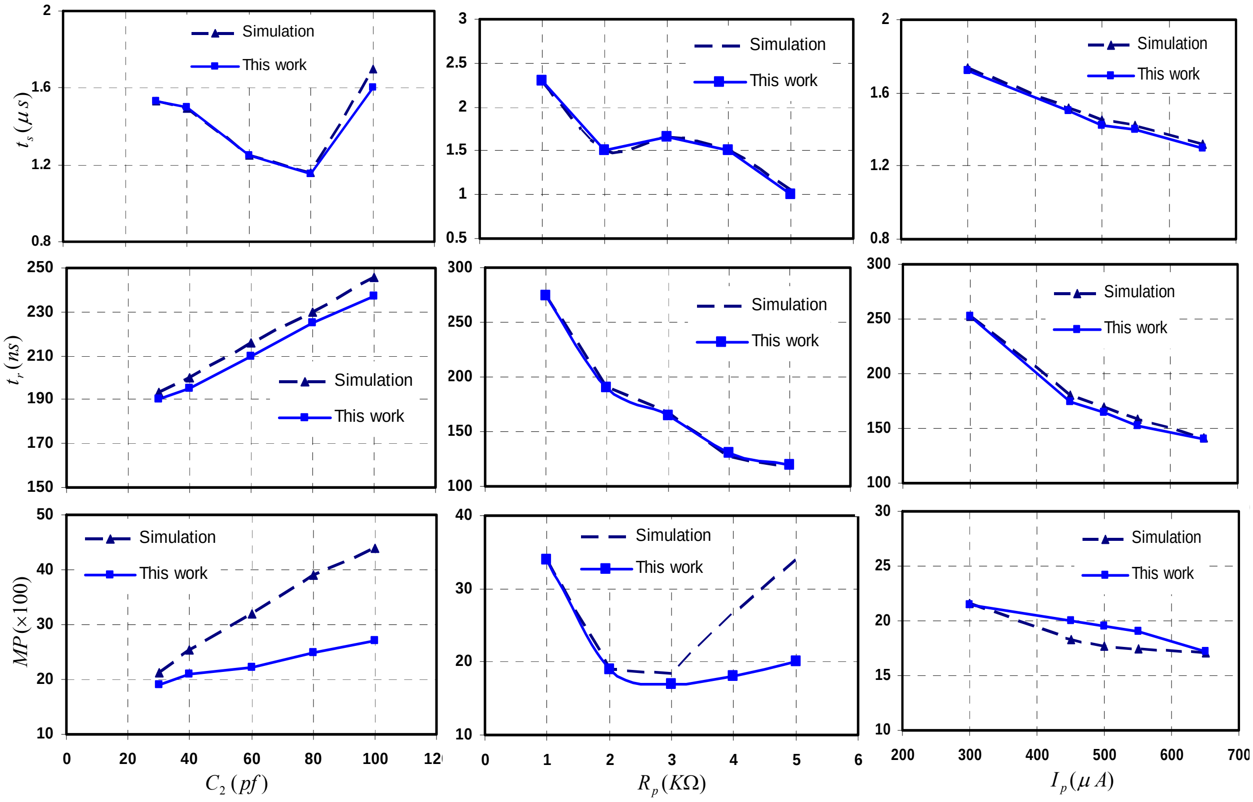

(a) (b) (c)

Fig. 6. Comparison between the simulated and calculated results of settling time, rise time and overshoot versus (a) C_p (b) R_p (c) I_p

Comparison between simulations and the results obtained from the proposed method are shown in Fig. 6.

For different values of loop parameters, the phase margin is obtained from (6). Table 2 summarizes the phase margin of system for different values of loop parameters. Overall, the results indicate that when the loop stability or phase margin are decreased, then, the accuracy of the proposed approach for the calculation of maximum overshoot will be degraded but the settling time and rise time are proper. Simulations show if the ratio C_p/C_2 is decreased, the loop stability is reduced which can be confirmed from (6) and (7).

As seen, simulation results of the above example indicate that the proposed approximation approach provides reasonable accuracy and very suitable while carrying an intuitive view of the transient behavior.

Table 1. Transient response simulation parameters of the example

	3rd PLL step response	Approximated step response
t_d	-	-6.97e-8
a_0	-	1.67e13
a_1	-	1e7
α	-	4.44e6
ω_d	-	1.72e6
θ (rad)	-	-0.31
β	-	-0.32
t_p (ns)	506	491
M_p (%)	18.7%	19%
ξ	-	0.4
t_r (ns)	190	190
t_s (ns)	1.5	1.5
PM	60˚	59˚

Table 2. The phase margin of system for different values of loop parameters

(1)	I_p=420μA, C_p=300pf, R_p=2KΩ, K_{VCO}=50e6				
	C_2 (pf)				
	30	40	60	80	100
PM	56˚	51.8˚	44.7˚	39.6˚	35.7˚
(2)	I_p=420μA, C_p=300pf, C_2=100pf, K_{VCO}=50e6				
	R_p (KΩ)				
	1	2	3	4	5
PM	45.4˚	60˚	54˚	45˚	38˚
(3)	R_p=2KΩ, C_p=300pf, C_2=100pf, K_{VCO}=50e6				
	I_p (μA)				
	300	450	500	550	650
PM	58.9˚	60˚	59.7˚	59.3˚	58.2˚

6. CONCLUSION

The transient behavior of the third-order charge pump PLL was investigated in this paper. The presented analysis is carried out in the time domain, allowing a mathematical modeling of the transient response in PLL. The proposed approach is used for approximated analysis and predicting the loop transient specification such as damping ratio, overshoot, settling time and other parameters for the PLL. Finally, behavioral simulations in MATLAB indicate exact agreement between the simulated results of the actual PLL and the proposed approximated approach. The results in this work help designers to estimate and optimize the performance of the third-order PLL in system-level design.

REFERENCES

[1] I. Young, J. Greason, and K. Wong, “**PLL clock generator with 5 to 10MHz of lock range for microprocessors**,” *IEEE J. Solid-State Circuits*, Vol. 27, No.11, pp. 1599-1607, Nov. 1992.

[2] H. Adrang, H. Miar Naimi, “**Modeling of Jitter in Bang-Bang CDR with Fourier Series Analysis**”, *IEEE Transactions on Circuits and Systems I*, Vol. 60, No. 1, pp. 3-10, Jan. 2013.

[3] Dong Jiao, Bongjin Kim, Kim, C.H., “**Design, Modeling, and Test of a Programmable Adaptive Phase-Shifting PLL for Enhancing Clock Data Compensation**”, *IEEE J. Solid-State Circuits*, Vol. 47, No. 10, pp. 1634-1639, Oct. 2012.

[4] H. Rategh, H. Samavati, and T. Lee, “**A CMOS frequency synthesizer with an injection-locked frequency divider for a 5-GHz wireless LAN receiver,**” *IEEE J. Solid-State Circuits*, Vol. 35, No. 5, pp. 780-787, May 2000.

[5] A. Ebrahimi, H. Miar Naimi, H. Adrang, “**Remarks on Transient amplitude analysis of CMOS cross-coupled oscillator**”, *IEICE Transactions on Electronics*, Vol. E94-C, No. 2, pp. 231-239, Feb. 2011.

[6] S. Aouini, K. Chuai; G. W. Roberts, “**Anti-Imaging Time-Mode Filter Design Using a PLL Structure With Transfer Function DFT**”, *IEEE Transactions on Circuits and Systems I,* Vol. 59, No.1, pp. 66-79, Jan. 2012.

[7] A. Ebrahimi, and H. Miar Naimi, "**Analytical Equations for Amplitude Analysis of MOS Colpitts Oscillator,**" *International Journal of Electronics*, Vol. 98, No. 7, pp. 883-900, July 2011.

[8] A. Ebrahimi and H. Miar Naimi, “**An improvement on the analytical methods for amplitude analysis of the MOS Colpitts oscillator**” in *2010 XIth International Workshop on Symbolic and Numerical Methods, Modeling and Applications to Circuit Design (SM2ACD)*, Oct. 2010.

[9] S. Miyazawa, R. Horita, K. Hase, K. Kato, and S. Kojima, “**A BiCMOS PLL-based data separator circuit with high stability and accuracy**,” *IEEE J. Solid-State Circuits*, Vol. 26, No. 2, pp. 116-121, Feb. 1991.

[10] J. Hein and J. Scott, “**z-domain model for discrete-time PLLs**,” *IEEE Trans. Circuits Syst.*, Vol. 35, No. 11, pp. 1393-1400, Nov. 1988.

[11] F. Gardner, “**Charge pump phase-lock loops,**” *IEEE Trans*. Commun., Vol. COM-28, pp. 1849-1858, Nov 1980.

[12] I. Novof, J. Austin, R. Kelkar, D. Strayer, and S. Wyatt, “**Fully integrated CMOS phase-locked loop with 15 to 240 MHz locking range and ±50 ps jitter,**” *IEEE J. Solid-State Circuits*, Vol. 30, No. 11, pp. 1259-1266, Nov. 1995.

[13] J. Maneatis, “**Low-jitter process-independent DLL and PLL based on self-biased techniques**,” *IEEE J. Solid-State Circuits*, Vol. 31, No. 11, pp. 1723-1732, Nov. 1996.

[14] L. A. H. Monterio D. N. Favaretto Filho, and J. R. C. Piqueira, “**Bifurcation Analysis for Third-Order Phased-Locked Loops**,” *IEEE signal processing letters*., Vol. 1, No. 5, pp. 494-496 , May. 2004.

[15] A. Carlosena, M. Ugarte, A. J. López-Martín, “**Loop Filter Approximation for PLLs**”, *IEEE MWSCAS*, 2008, pp. 21-24.

[16] A. Carlosena, A. M. Lazaro, "**A Novel Design Method for Phased-Locked Loops of any Order and Type,**" *IEEE MWSCAS*, 2006, pp. 569-573.

[17] H. Adrang, "**A systematic procedure for analysis of third-order charge pump phase-locked loop (PLL),**" Scientific Research and Essays, Vol. 7, No. 2, pp. 190-198, Jan. 2012.

[18] H. Adrang and H. M. Naimi, "**A Novel Method for Analysis and Design of Third-Order Charge Pump PLL,**" *IEEE ECCTD Conference*, pp. 591-594, 2009.

[19] C. Cao, Y. Ding and K. O. Kenneth, "**A 50-GHz Phase Locked Loop in 0.13-μm CMOS,**" *IEEE Journal of Solid-State Circuits*, Vol. 42, No. 8, pp. 1649-1656, Aug. 2007.

[20] J. R. Smith, "**Modern Communication Circuits,**" *New York. McGraw-Hill*, 1997.

[21] K. Ogata, "**Modern Control Engineering,**" *Pearson Education. 2001*.